

UCSF

UC San Francisco Previously Published Works

Title

Coaxial flow focusing in poly(dimethylsiloxane) microfluidic devices

Permalink

<https://escholarship.org/uc/item/8f129488>

Journal

Biomicrofluidics, 8(1)

ISSN

1932-1058

Authors

Tran, Tuan M
Cater, Sean
Abate, Adam R

Publication Date

2014

DOI

10.1063/1.4863576

Peer reviewed

Coaxial flow focusing in poly(dimethylsiloxane) microfluidic devices

Tuan M. Tran,¹ Sean Cater,² and Adam R. Abate^{2,a)}

¹Joint UCSF/UCB Bioengineering Graduate Group, University of California, San Francisco 1700, 4th Street, Byers Hall 303C, San Francisco, California 94158, USA

²Department of Bioengineering and Therapeutic Sciences, California Institute for Quantitative Biosciences (QB3), University of California, San Francisco 1700, 4th Street, Byers Hall 303C, San Francisco, California 94158, USA

(Received 6 September 2013; accepted 17 January 2014; published online 3 February 2014; corrected 19 February 2014)

We have developed a coaxial flow focusing geometry that can be fabricated using soft lithography in poly(dimethylsiloxane) (PDMS). Like coaxial flow focusing in glass capillary microfluidics, our geometry can form double emulsions in channels with uniform wettability and of a size much smaller than the channel dimensions. However, in contrast to glass capillary coaxial flow focusing, our geometry can be fabricated using lithographic techniques, allowing it to be integrated as the drop making unit in parallel drop maker arrays. Our geometry enables scalable formation of emulsions down $7\ \mu\text{m}$ in diameter, in large channels that are robust against fouling and clogging. © 2014 AIP Publishing LLC.

[<http://dx.doi.org/10.1063/1.4863576>]

I. INTRODUCTION

Double emulsions consist of droplets that contain smaller droplets in their bulk and have many applications for research and industry. For example, in research, double emulsions serve as templates for polymer capsules, core-shell particles, and non-spherical particles.¹ In industry, double emulsions are being developed as delivery vehicles for active compounds, like pesticides, cosmetic agents, and drugs. By encapsulating active compounds in double emulsions, they can be dispersed into environments in which they are poorly soluble, protected from degradation, and controllably released to achieve uniform dosing.²⁻⁷

Controlling the performance characteristics of double emulsions requires precise control of their structural properties. The best method for forming double emulsions with controlled structure is coaxial flow focusing, a technique pioneered in glass capillary microfluidics.⁸ In this technique, the inner and middle phases of the double emulsion are sheared into monodisperse droplets by focusing them through a small orifice. By adjusting flow conditions and orifice dimensions, it is possible to form double emulsions over a broad range of dimensions and morphologies.⁹ Coaxial flow focusing also has benefits for industrial applications: Because the inner and middle phases are centered in the orifice and protected from the channel walls by the encapsulating sheath fluid, fouling by dissolved compounds is minimized, allowing the device to operate for long periods without interruption. In addition, coaxial flow focusing can generate droplets much smaller than the focusing orifice. Without coaxial flow focusing, forming drops $<10\ \mu\text{m}$ in diameter requires channels smaller than this size.^{10,11} Thus, coaxial flow focusing is valuable for forming emulsions $<10\ \mu\text{m}$ in diameter, because the large channels it uses are easier to fabricate and more robust against clogging.¹²

The primary disadvantage of coaxial flow focusing is that it requires the fabrication of microfluidic devices with channels that constrict in the horizontal and vertical planes. While methods to make multilayer droplet generation devices in poly(dimethylsiloxane) (PDMS) have been

^{a)}E-mail: adam.abate@ucsf.edu

developed for both emulsification and laminar flow mixing, such devices do not employ coaxial flow focusing to generate emulsions smaller than the nozzle size.^{10,13–15} To date, coaxial flow focusing geometries have only been fabricated with glass capillaries or multiple layers of SU-8.^{16,17} While these devices are capable of forming double emulsions with controlled properties, they are difficult to replicate. Glass capillary devices require manual tip shaping and alignment of each device, while multilayer SU-8 devices require long cycles of spin coating, baking, exposure, and alignment.^{17,18} In addition, both methods yield one device per fabrication, whereas, with soft lithography, a single master can be used to replicate hundreds of exact copies, making the approach scalable. To enable the generation of double emulsions of the desired size and in a format that is scalable, a new approach is needed that combines the optimal flow characteristics of coaxial flow focusing with the scalability of devices fabricated using soft lithography.

In this paper, we introduce coaxial flow focusing in lithographically-fabricated PDMS devices. Just as in glass capillary microfluidics, our geometry focuses the fluids through a constriction that narrows in the horizontal and vertical planes. As such, our device shares many of the advantages of capillary coaxial flow focusing: Because the walls are protected by the sheath flow of the carrier phase, channel wettability is unimportant with respect to the kinds of emulsions that can be formed, allowing us to form o/w single emulsions and w/o/w double emulsions in channels that are uniformly hydrophobic. The sheath flow also minimizes contact of the phases with the channel walls, reducing fouling. Moreover, just like coaxial flow focusing in glass capillaries, our geometry forms double emulsions smaller than the orifice, allowing droplets $<10\ \mu\text{m}$ in diameter to be generated in channels $50\ \mu\text{m}$ in size. Last, and perhaps most important, our geometry is fabricated in PDMS using an entirely lithographic process and, thus, can be integrated as the drop making unit in parallel drop maker arrays. PDMS is the dominant polymer used in microfluidics, allowing our method to be widely adopted. In addition, the same molding technique used to fabricate our coaxial flow focusing geometry in PDMS can also be extended to other materials, like photopolymerizable epoxies or plastic devices constructed with hot embossing or injection molding. Combined, these properties should allow the scalable production of double emulsions of the desired small size in device arrays that are robust against fouling and clogging.

II. EXPERIMENTAL

A. Preparation of devices

To fabricate our coaxial flow focusing geometry, we use multi-level photolithography,^{19,20} which allows us to create channels with constrictions in the x-y and y-z planes. To fabricate these devices, we use two masters (Figure S1).²¹ One master contains the $50\ \mu\text{m}$ tall features for the first cross junction and constriction and $185\ \mu\text{m}$ tall features for the large channels of the second junction. The second master contains a $135\ \mu\text{m}$ mirror-image of just the $185\ \mu\text{m}$ channels.

To construct the finished drop maker, the two masters are used to mold separate PDMS devices. The PDMS devices are sliced and peeled from the masters and the inlet ports are punched into them. The PDMS devices are washed with isopropanol and plasma oxidized to ready them for alignment and bonding. To bond the devices, a droplet of water is placed onto the PDMS slab containing $135\ \mu\text{m}$ channels, with the channels face-up. The slab containing the 50 and $185\ \mu\text{m}$ layers is then placed onto the first slab face down, so that the $135\ \mu\text{m}$ and $185\ \mu\text{m}$ channels align as mirror images. To align the slabs with high precision, we implement mechanical alignment “frames” consisting of $50\ \mu\text{m}$ protruding ridges on the upper slab and $50\ \mu\text{m}$ recessed channels on the lower slab, which lock into place when the two slabs are precisely aligned. The water droplet lubricates the slabs, allowing them to slide until the mechanical alignment lock is achieved. We use water because it is an effective lubricant for the hydrophilic plasma treated surfaces and also because it does not reduce the strength of the plasma bond. To evaporate the water and allow the two surfaces to fully bond, the aligned devices are baked for two days at 60°C . During this time, the channels revert to their native hydrophobic state, which is necessary for our device to form water-in-oil-in-water double emulsions. While PDMS is optically transparent, the thickness of the lower layer of the device may limit high resolution imaging in the channels for certain applications.²²

B. Preparation of emulsions

To generate double emulsions, we use distilled water for the inner phase, Novec 7500 fluorinated oil with 1 wt. % biocompatible surfactant for the middle phase,²³ and a 10 wt. % polyethylene glycol (PEG) solution containing 1 wt. % Tween 20 and 1 wt. % sodium dodecyl sulfate (SDS) for the continuous phase. The viscosities of the solutions are: $7.7 \times 10^{-7} \text{ m}^2 \text{ s}^{-1}$ for Novec 7500, $1.01 \times 10^{-6} \text{ m}^2 \text{ s}^{-1}$ for water, and $\geq 6 \times 10^{-6} \text{ m}^2 \text{ s}^{-1}$ for the PEG solution.²⁴ The surface tension between the water phases and the oil is estimated to be between $0.002\text{--}0.005 \text{ N m}^{-1}$.²⁵ The PEG increases the viscosity of the continuous phase, allowing us to achieve higher shears in the second junction with lower flow rates, making it easier to form the emulsions.

C. Flow rate estimation for single emulsions

To achieve the wide range of single emulsion drop sizes, we wanted a low flow rate of the inner phase. At low flow rates, syringe pumps tend to have lower accuracy. Therefore, our desired inner phase flow rate of $20 \mu\text{l/h}$ on our control software did not match the actual inner phase flow rate. To determine the actual flow rate of single emulsions, we used the double emulsion images to obtain an equation relating flow rate to the measured jet diameter

$$Q_{sum} = \frac{Q_C}{\frac{16WH}{9\pi D_{jet}} + 1}, \quad (1)$$

where D_{jet} is the diameter of the jet, Q_{sum} is the sum of the inner and middle phase flow rates, Q_C is the continuous phase flow rate, and W and H are the width and height of the constriction, respectively. Equation (1) is derived from assuming a parabolic flow profile in a rectangular channel and is an approximation of the flow profile since the two jets may not form a continuous parabola. However, we can still obtain an accurate prediction of flow rate by adjusting H to match our double emulsion flow rate data. We then use Eq. (1) to calculate the flow rate of Q_{sum} for single emulsions and obtain an average value of $Q_{sum} = 118 \mu\text{l/h}$, which we use for the remainder of our analysis.

III. RESULTS AND DISCUSSION

A. Microfluidic design and operation

Our coaxial flow focusing geometry employs a 3-dimensional channel layout (Figure 1). The inner phase is first combined with the middle phase in a $10 \times 50 \mu\text{m}$ cross junction.

Due to the hydrophobicity of the channels, the oil phase lifts the aqueous phase off of the channels and surrounds it, forming a long jet that flows into the second junction. In the second

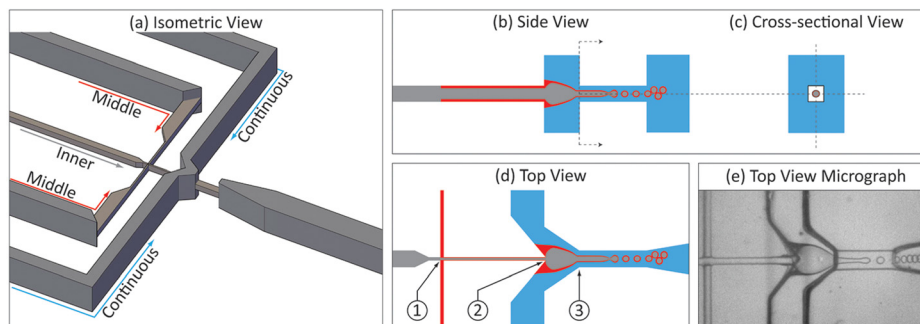


FIG. 1. (a) Isometric view of lithographically-fabricated coaxial flow focusing device, with phases labelled. (b) Side view of channels with inner (grey), middle (red), and continuous (blue) phases indicated. (c) Cross sectional view showing the square orifice enabling flow focus drop formation. (d) Schematic diagram and (e) microscope image of top view of device showing flow focus drop formation. At junction (1), the inner and middle phases combine. At junction (2), the channel expands, and the inner and middle phases combine with the continuous phase, creating the double jet. At junction (3), the double jet is focused through the orifice, generating double emulsions.

junction, the channels abruptly increase in height to $320\ \mu\text{m}$, and a second aqueous phase is injected, as illustrated in Figures 1(b) and 1(c). The abrupt expansion of the channels and high velocity of the outer aqueous fluid lifts the oil from the channel walls. This creates a double jet consisting of the inner jet of aqueous fluid sheathed in a thin shell of oil, surrounded by the second aqueous phase, as illustrated in Figures 1(b) and 1(d). The double jet is then focused through a small “orifice” consisting of a $50 \times 50\ \mu\text{m}$ channel constriction, as shown from different perspectives in the panels in Figure 1. The constriction causes the velocity of the continuous phase to increase, generating high shears that rip droplets from the end of the jet, as illustrated

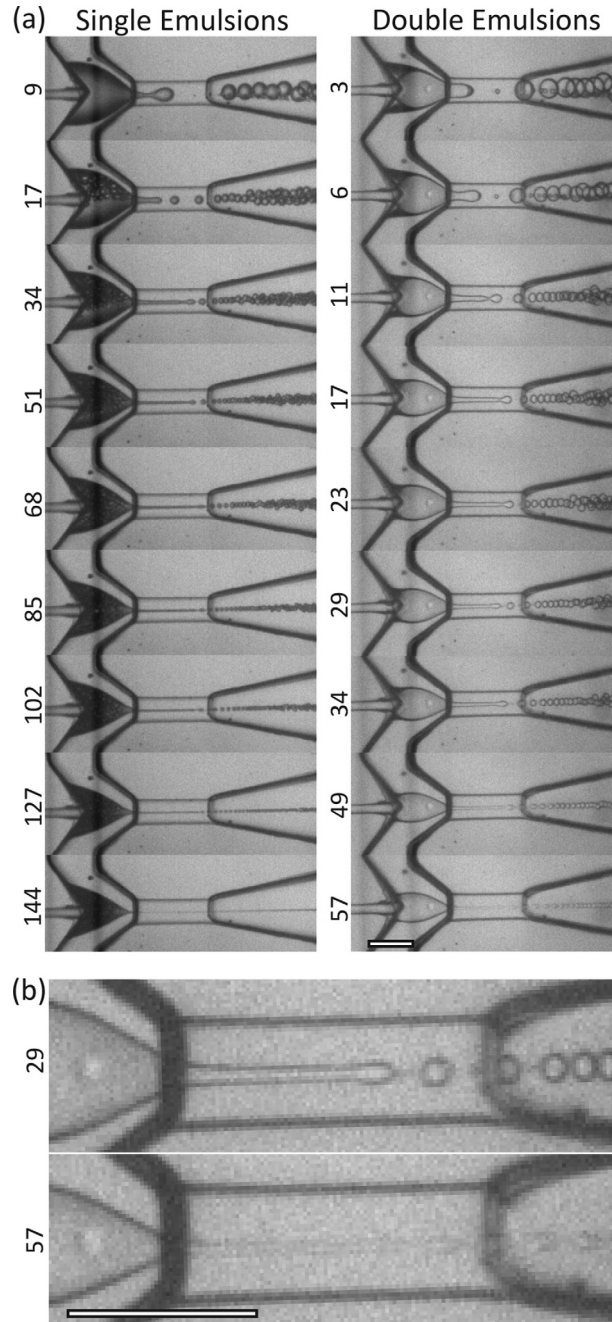


FIG. 2. (a) Generation of single (left) and double (right) emulsions at different flow rates. The number labels correspond to the Q_C/Q_{sum} values. $Q_{sum} = 118$ and $350\ \mu\text{l/h}$ for single and double emulsions, respectively. (b) Magnified images of double emulsion drop formation with Q_C/Q_{sum} values to the left. The scale bar denotes $100\ \mu\text{m}$.

in Figure 1(e). This process resembles the generation of double emulsions with coaxial flow focusing in glass capillary devices, except that the channels have rectangular cross sections rather than round ones.

B. Flow focused formation of single and double emulsions

The coaxial geometry of our device allows us to generate single and double emulsions over a wide range of sizes and flow rates (Figure 2). It also allows us to generate drops substantially smaller than the constriction orifice. For the single emulsions, we form drops smaller than the pixel size in our image, which is $2\ \mu\text{m}$. However, we omitted the resolution limited data from our analysis, since an accurate estimate of the error is difficult to obtain (Figure S2).²¹ For the double emulsions, we form drops down to $14\ \mu\text{m}$ in diameter. To characterize the uniformity of the emulsions generated by our device, we measure the coefficient of variation (CV) of the droplet diameters. For the double emulsions, we measure a CV of 5.2% and for single emulsions 5.6%.

Our geometry mimics the flow focusing geometry of microcapillary devices, except that rather than a round orifice, the orifice of our device is rectangular. In a round orifice, the velocity profile is axisymmetric, whereas it is not axisymmetric in a square channel.²⁶ However, previous studies have shown the dripping and jetting regimes of jets in square channels and cylindrical channels generally agree for jets unconfined by the square channel walls, which is the case for our device too.^{27,28} In addition, for square channels, the scaling laws for drop size based on inner and outer flow rates are similar for unconfined drops.²⁹ Therefore, our device should form double emulsions through the same mechanism as microcapillaries. If so, the scaling of drop size as a function of flow rate should be similar. To confirm whether this is the case, we vary flow rates and measure the corresponding change in drop size. We find that, just as in glass capillary devices, increasing the ratio of continuous phase to the inner and middle phases yields smaller drops, see Figure 3. In glass capillary devices,

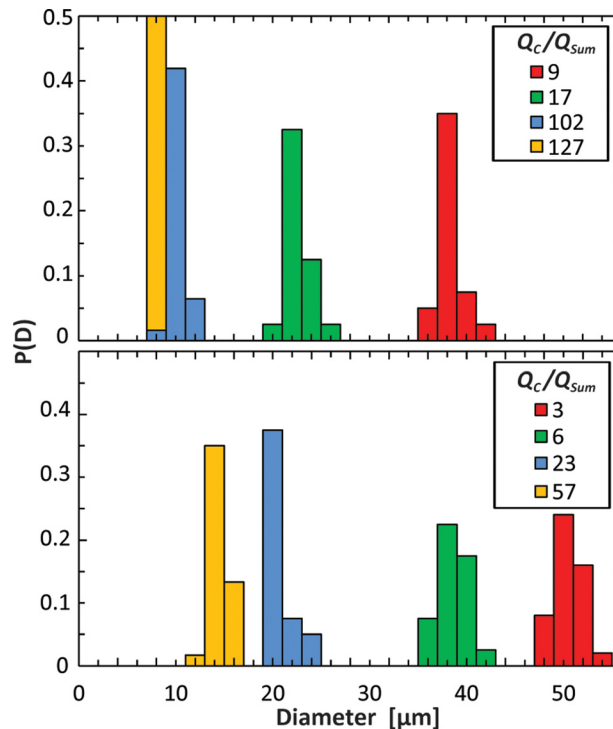


FIG. 3. Histograms of drop sizes for single (top) and double (bottom) emulsions for different flow rates.

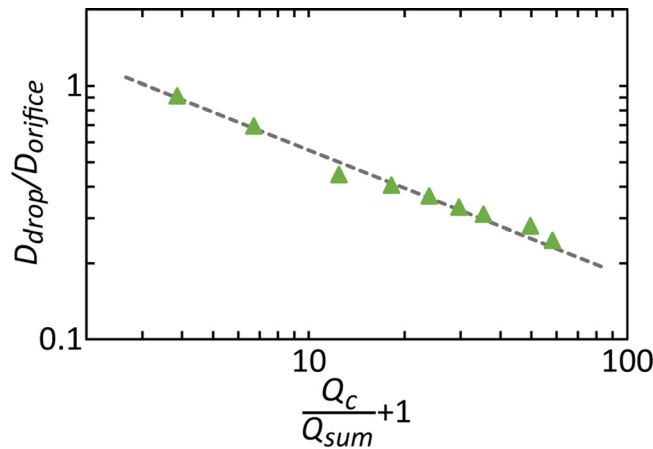


FIG. 4. Droplet diameter versus flow rate ratio $Q_c/Q_{sum} + 1$ for double emulsions. The dotted line corresponds to the best fit of Eq. (1) for the double emulsions, which yields $C = 1.77 \pm 0.07$.

$$\frac{D_{drop}}{D_{orifice}} = C \left(\frac{Q_c}{Q_{sum}} + 1 \right)^{-\frac{1}{2}}, \quad (2)$$

where $D_{orifice}$ is the width of the flow focusing orifice, and C is a fitted parameter related to λ , the most unstable perturbation wavelength of the jet.³⁰ To compare our data with this functional form, we plot the scaled double emulsion drop size as a function of flow rates in Figure 4 and fit Eq. (2) by adjusting C . By fitting our double emulsion data, we obtain $C = 1.77 \pm 0.07$. This C value agrees with $C = 1.87$ from previous double emulsion results for glass capillary devices.⁸ Our data is thus remarkably well described by the equation, suggesting that the mechanism of drop formation in our lithographically-fabricated device is similar to that of glass capillary devices.

IV. CONCLUSION

We have demonstrated the generation of single and double emulsions using coaxial flow focusing in a lithographically-fabricated device. Our device combines the ability to form small, monodisperse emulsions of glass capillary flow focusing with the scalability of devices fabricated lithographically. The devices can be readily parallelized by fabricating them in an array format and using published methods for distributing fluids evenly to the double emulsification junctions. This should allow the droplet generation rates to increase by several orders of magnitude, allowing scalable generation of small, monodisperse double emulsions. In addition, the ability to form small double emulsions in large coaxial flow focusing channels should make the device resistant to fouling and clogging, which is critical when parallelizing the devices intended to run for long durations without intervention.

ACKNOWLEDGMENTS

This work was supported by a Research Award from the California Institute for Quantitative Biosciences (QB3), the Bridging the Gap Award from the Rogers Family Foundation, the UCSF/Sandler Foundation Program for Breakthrough Biomedical Research, a grant from BASF, and the NSF through the Faculty Early Career Development (CAREER) Program (DBI-1253293).

¹C. A. Serra and Z. Chang, *Chem. Eng. Technol.* **31**, 1099 (2008).

²C. Laugel, A. Baillet, M. P. Y. Piemi, J. P. Marty, and D. Ferrier, *Int. J. Pharm.* **160**, 109 (1998).

³D. Lee and D. A. Weitz, *Adv. Mater.* **20**, 3498 (2008).

⁴M.-H. Lee, S.-G. Oh, S.-K. Moon, and S.-Y. Bae, *J. Colloid Interface Sci.* **240**, 83 (2001).

⁵C. Lobato-Calleros, E. Rodriguez, O. Sandoval-Castilla, E. J. Vernon-Carter, and J. Alvarez-Ramirez, *Food Res. Int.* **39**, 678 (2006).

- ⁶D. Vasiljevic, J. Parojcic, M. Primorac, and G. Vuleta, *Int. J. Pharm.* **309**, 171 (2006).
- ⁷J. Weiss, I. Scherze, and G. Muschiolik, *Food Hydrocolloids* **19**, 605 (2005).
- ⁸A. S. Utada, E. Lorenceau, D. R. Link, P. D. Kaplan, H. A. Stone, and D. A. Weitz, *Science* **308**, 537 (2005).
- ⁹L.-Y. Chu, A. S. Utada, R. K. Shah, J.-W. Kim, and D. A. Weitz, *Angew. Chem. Int. Ed.* **46**, 8970 (2007).
- ¹⁰A. Rotem, A. R. Abate, A. S. Utada, V. Van Steijn, and D. A. Weitz, *Lab Chip* **12**, 4263 (2012).
- ¹¹C. Holtze, *J. Phys. D: Appl. Phys.* **46**, 114008 (2013).
- ¹²R. K. Shah, J.-W. Kim, J. J. Agresti, D. A. Weitz, and L.-Y. Chu, *Soft Matter* **4**, 2303 (2008).
- ¹³M. E. Brennich, J.-F. Nolting, C. Dammann, B. Nöding, S. Bauch, H. Herrmann, T. Pfohl, and S. Köster, *Lab Chip* **11**, 708 (2011).
- ¹⁴M. E. Kinahan, E. Filippidi, S. Kouster, X. Hu, H. M. Evans, T. Pfohl, D. L. Kaplan, and J. Wong, *Biomacromolecules* **12**, 1504 (2011).
- ¹⁵H. Y. Park, X. Qiu, E. Rhoades, J. Korlach, L. W. Kwok, W. R. Zipfel, W. W. Webb, and L. Pollack, *Anal. Chem.* **78**, 4465 (2006).
- ¹⁶R. K. Shah, H. C. Shum, A. C. Rowat, D. Lee, J. J. Agresti, A. S. Utada, L.-Y. Chu, J.-W. Kim, A. Fernandez-Nieves, C. J. Martinez, and D. A. Weitz, *Mater. Today* **11**, 18 (2008).
- ¹⁷S.-H. Huang, W.-H. Tan, F.-G. Tseng, and S. Takeuchi, *J. Micromech. Microeng.* **16**, 2336 (2006).
- ¹⁸A. R. Abate, D. Lee, C. Holtze, A. Krummel, and W. D. Do, *Lab—Chip Technol. Fabr. Microfluid* (Caister Academic Press, 2009).
- ¹⁹F.-C. Chang and Y.-C. Su, *J. Micromech. Microeng.* **18**, 065018 (2008).
- ²⁰M. B. Romanowsky, A. R. Abate, A. Rotem, C. Holtze, and D. A. Weitz, *Lab Chip* **12**, 802 (2012).
- ²¹See supplementary material at <http://dx.doi.org/10.1063/1.4863576> for Figures S1 and S2 (n.d.).
- ²²S. Pennathur and D. K. Fygenson, *Lab Chip* **8**, 649 (2008).
- ²³B. O'Donovan, D. J. Eastburn, and A. R. Abate, *Lab Chip* **12**, 4029 (2012).
- ²⁴L. Ninni, H. Burd, W. H. Fung, and A. J. A. Meirelles, *J. Chem. Eng. Data* **48**, 324 (2003).
- ²⁵A. R. Abate, A. Poitzsch, Y. Hwang, J. Lee, J. Czerwinska, and D. A. Weitz, *Phys. Rev. E* **80**, 026310 (2009).
- ²⁶A. S. Utada, A. Fernandez-Nieves, H. A. Stone, and D. A. Weitz, *Phys. Rev. Lett.* **99**, 094502 (2007).
- ²⁷J. K. Nunes, S. S. H. Tsai, J. Wan, and H. A. Stone, *J. Phys. D: Appl. Phys.* **46**, 114002 (2013).
- ²⁸P. Guillot, A. Colin, and A. Ajdari, *Phys. Rev. E* **78**, 016307 (2008).
- ²⁹T. Cubaud and T. G. Mason, *Phys. Fluids* **20**, 053302 (2008).
- ³⁰S. Tomotika, *Proc. R. Soc. London, Ser. A* **150**, 322 (1935).